Ocean Dynamics
DOI 10.1007/s10236-010-0370-7

Sediment mobility in response to tidal and wind-driven flows along the Belgian inner shelf, southern North Sea

Matthias Baeye · Michael Fettweis · George Voulgaris · Vera Van Lancker

Received: 27 September 2010 / Accepted: 8 December 2010

Abstract The effect of hydro-meteorological forcings (tidal and wind-induced flows) on the transport of suspended particulate matter (SPM), on the formation of high-concentrated mud suspensions and on the occurrence of sand–mud suspensions has been studied using long-term multi-parametric observations. Data have been collected in a coastal turbidity maximum area (southern North Sea) where a mixture of sandy and muddy sediments prevails. Data have been classified according to variations in subtidal alongshore currents, with the direction of subtidal flow depending on wind direction. This influences the position of the turbidity maximum; as such also the origin of SPM. Winds blowing from the NE will increase SPM concentration, whilst SW winds will induce a decrease. The latter is related to advection of less turbid English Channel water, inducing a shift of the turbidity maximum towards the NE and the Westerschelde estuary. Under these conditions, marine mud will be imported and buffered in the estuary. Under persistent NE winds, high-concentrated mud suspensions are formed and remain present during several tidal cycles. Data show that SPM consists of a mixture of flocs and locally eroded sand grains during high currents. This has implications towards used instrumentation: SPM concentration estimates from optical backscatter sensors will only be reliable when SPM consists of cohesive sediments only; with mixtures of cohesive and non-cohesive sediments, a combination of both optical and acoustic sensors are needed to get an accurate estimate of the total SPM concentration.

Keywords Suspended particulate matter · Mixed sediments · High-concentrated mud suspensions · Alongshore sediment transport · Acoustic and optical backscattering · Southern North Sea

Responsible Editor: Aida Alvera-Azcárate

M. Baeye (✉)
Department of Geology and Soil Science,
Renard Centre of Marine Geology (RCMG), Ghent University,
Ghent 9000, Belgium
e-mail: Matthias.baeye@ugent.be

M. Fettweis · V. Van Lancker
Management Unit of the North Sea Mathematical Models (MUMM), Royal Belgian Institute of Natural Sciences,
Brussels 1200, Belgium

G. Voulgaris
Department of Earth and Ocean Sciences,
University of South Carolina,
Columbia, SC 29208, USA

1 Introduction

In coastal areas, benthic sediments generally consist of sand and mud mixtures. The mud/sand ratio influences the transition between cohesive and non-cohesive sediments and has a major influence on the erosion behaviour, on suspended particulate matter (SPM) concentration and on the benthic ecological properties (Williamson and Torfs 1996; Torfs et al. 1996; Panagiotopoulos et al. 1997; Wallbridge et al. 1999; Flemming and Delafontaine 2000; van Ledden et al. 2004; Waeles et al. 2007; Van Hoey et al. 2007). Frequently, mixed sediments occur as an alternation of sand and mud layers. Fan et al. (2004) describe storm-induced waves as randomly occurring erosive forces on the

Published online: 07 January 2011

sediment bed, producing intense sediment mobilization leading to the deposition of sand-dominated layers. This type of vertical segregation within the sedimentary record can only occur, if cohesive SPM concentration is relatively low. In case of high SPM concentration, the segregation in sand/mud suspensions occurs when the initial mud concentration is smaller than its gelling point (Torfs et al. 1996). Cohesive SPM dynamics are complex and are affected by hydrodynamics, waves, wind, local and remote sediment availability (i.e., SPM sources), bed composition, biological processes and human impact (Le Bot et al. 2010; Van Lancker et al. 2010). Furthermore, in high-turbidity areas fluid mud layers may be formed. Fluid mud is a high concentration suspension of fine-grained sediment in which settling is substantially hindered. Fluid mud consists of water, clay-sized particles and organic materials; it displays a variety of rheological behaviours ranging from elastic to pseudo-plastic (McAnally et al. 2007). Massive sedimentation of fine-grained sediments in harbours and navigation channels is often related with the occurrence of fluid mud layers (Verlaan and Spanhoff 2000; Winterwerp 2005; PIANC 2008).

The inner shelf of the Belgian coast, located in the southern North Sea, is an example of an area where bed sediment composition varies from pure sand to pure mud (Verfaillie et al. 2006). It is characterized by elevated SPM concentrations (Fettweis et al. 2006) and has been the subject of high anthropogenic stresses due to harbour extension, dredging and disposal works, deepening of navigation channels and aggregate extraction (Lauwaert et al. 2009; Du Four and Van Lancker 2008; Van Lancker et al. 2010). Understanding of sediment distribution and mobility in such areas requires the use of multi-parametric observations. These should account for the mutual interaction of sand–mud mixtures as a function of bed armouring, size fraction, sheltering and exposure effects (Wiberg et al. 1994; Wallbridge et al. 1999; Wu et al. 2003).

With this scope in mind, in situ measurements of SPM concentration and characteristics, as also of currents have been carried out, using optical and acoustic sensors. This approach has already been successfully adopted in various mixed sediment environments (e.g. Thorne and Hanes 2002; Fugate and Friedrichs 2002; Voulgaris and Meyers 2004). The objective of this contribution is to identify the effects of the various hydrodynamic forcings (tidal and wind-induced flows) on suspended sediment transport and on the formation of high-concentrated mud suspensions (HCMS) and fluid mud layers. Furthermore, the forcing and sedimentary responses are analysed in terms of climatological parameters for the study site; as such, the findings can be used for developing an understanding of the long-term evolution of the system, and potentially for inclusion in future morphodynamic models.

2 Methodology

2.1 Study site

Situated in the southern North Sea (Fig. 1a), the Belgian nearshore is characterized by high-turbidity waters (Fig. 1b). Nearshore SPM concentration ranges between 20 and 70 mg l^{-1} and reaches 100 to >3.000 mg l^{-1} near the bed; lower values (<10 mg l^{-1}) occur offshore (Fettweis et al. 2010). The measurement station Blankenberge (BLA) is situated about 5 km SW of the port of Zeebrugge and is located on the eastern part of a shoreface-connected sand ridge (Fig. 1c). A coastal turbidity maximum zone (TMZ) is present between Oostende and the mouth of the Westerschelde (Fettweis et al. 2007). The BLA station is positioned in the TMZ. Sediment samples near BLA show variable sediment characteristics (fine sand, silt/clay), with a median grain size of the sand fraction of about 150 μm (Fig. 1c). Tidal regime is semi-diurnal and the mean tidal range at Zeebrugge is 4.3 and 2.8 m at spring and neap tide, respectively. A wind rose diagram (Fig. 2, left diagram) shows data over a 10-year period, collected at station MOW0 (3.5 km from BLA). Southwesterly winds dominate the overall wind climate, followed by winds from the NE sector. Maximum wind speeds coincide with the southwesterly winds; still, highest waves are generated under northwesterly winds.

2.2 Instrumentation

An instrumented tripod was deployed at a water depth of 5 m (location BLA, Fig. 1) to collect current, salinity and suspended sediment data. The instrumentation suite consisted of a 5 MHz SonTek^R Acoustic Doppler Velocimeter (ADVOcean-Hydra), a 3 MHz SonTek^R Acoustic Doppler Profiler (ADP), two D&A^R optical backscatter point sensors (OBS), Sea-bird^R SBE37 CT and a Sequoia Scientific^R Laser In Situ Scattering and Transmissometer 100-X (LISST-100X, Type-C). All data (except LISST) were stored in two SonTek^R Hydra data logging systems. The OBSs were mounted at 0.2 and 2 m above the bed (hereafter referred to as mab). The ADV velocities were measured at 0.2 mab, while the ADP profiler was attached at 2.3 mab and down-looking, measuring current and acoustic intensity profiles with a bin resolution of 0.25 m. Mean values were obtained once every 10 min for the OBS, LISST and ADV, while the ADP was set to record a profile every 1 min; later on averaging was performed to a 10-min interval to match the sampling interval of the other sensors. A total of 198 days of data have been collected, during five deployments, spanning autumn–winter 2006–2007, winter 2008 and spring 2008 (Table 1). The long deployments have ensured accurate sampling of condi-

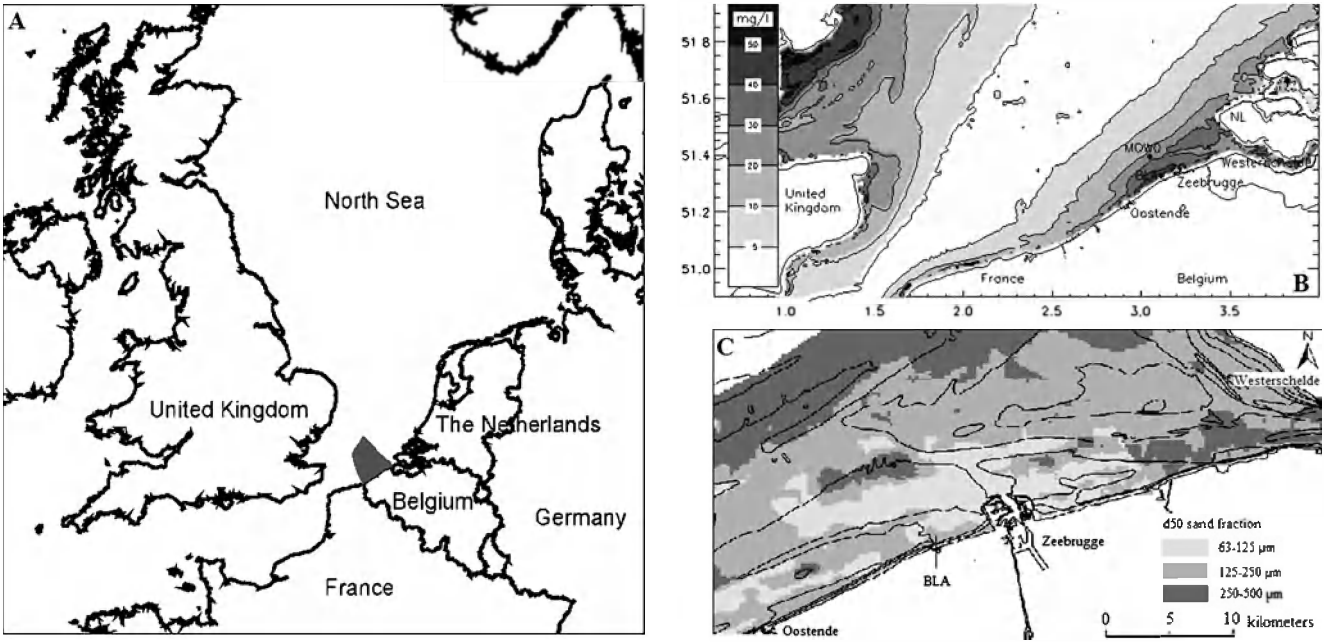

Fig. 1 **a** Map of southern North Sea, neighbouring countries and Belgian continental shelf (*grey area*); **b** map of the southern North Sea with the in situ SPM concentration measurement station BLA and the meteorological station MOW0. The background consists of the yearly averaged surface SPM concentration (mg·l^{-1}) from MODIS images (2003–2008); **c** map of d50 sand grain size (micrometre) in the region of interest (high-turbidity area between Oostende and the Westerschelde)

tions that include complete periods of neap and spring tides, as well as the occurrence of a variety of meteorological events.

The voltage of the OBS was converted to SPM concentration by calibration against filtered water samples during several field campaigns (Fettweis et al. 2006). A linear regression between all OBS signals and SPM concentrations from filtration was assumed. Data from the LISST 100C have been analysed only for the sediment grain size information.

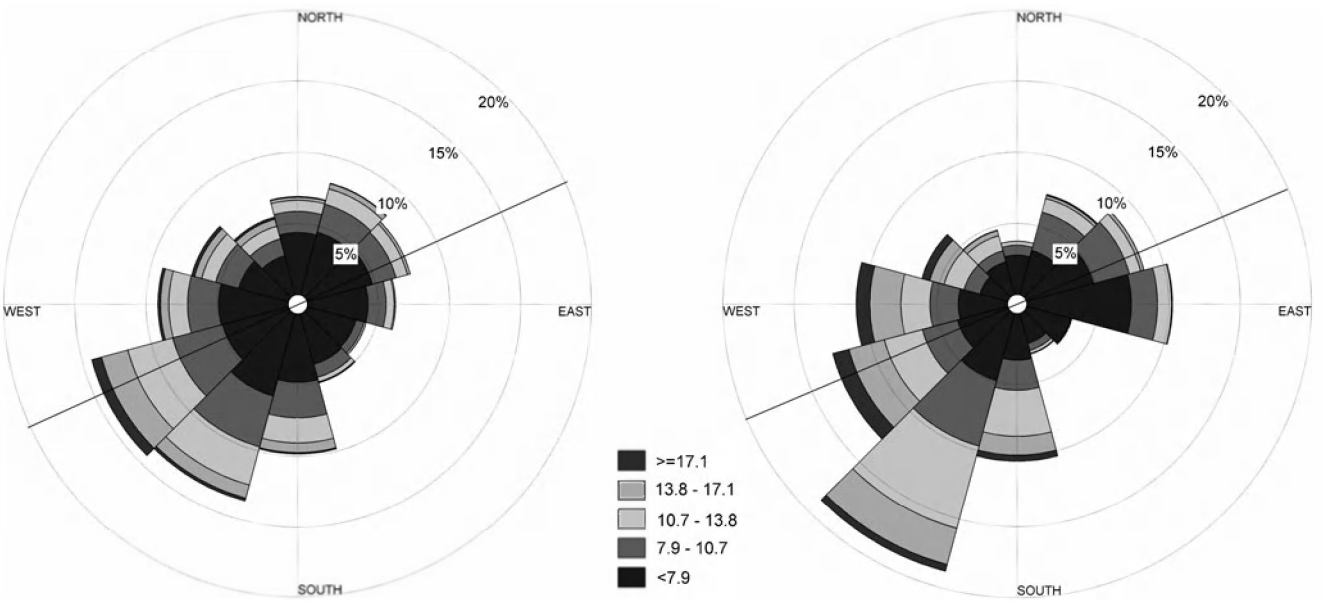

Fig. 2 Wind rose diagrams showing wind data over for 10 years (*left*) and wind data for the period of measurements (*right*). Legend values in m s^{-1}. *Black line* indicates coastline orientation at the measurement location (BLA)

Table 1 Tripod deployments at BLA site and the median and maximum significant wave height (H_s) during the measurement period

Start (dd/mm/yyyy hh:mm)	End ((dd/mm/yyyy hh:mm)	Duration (days)	Median (max) H_s (m)
8/11/2006 14:30	15/12/2006 08:30	36.7	0.83 (2.76)
18/12/2006 10:47	7/2/2007 13:17	50.1	0.79 (2.96)
28/01/2008 15:38	24/02/2008 13:18	26.9	0.44 (2.82)
6/3/2008 9:09	8/4/2008 15:29	33.7	0.76 (3.03)
15/04/2008 08:58	5/6/2008 7:48	51	0.46 (1.69)

Besides time series of current velocities and acoustic amplitude, the ADV was configured to also measure and store the distance between sensor and boundary (i.e. sea bed). The altimetry of the ADV was used to detect variation in bed level, as also for the identification of deposition and resuspension of fine-grained sediments. For the study site, decreasing distance between probe and bed boundary can correspond to the presence of HCMS acting as an acoustic reflector. However, the boundary detection may fail, due to attenuation of the signal (Velasco and Huhta 2010).

2.3 Analysis of data

Current time series (ADV and ADP) were filtered for the tidal signal using a low-pass filter for periods less than 33 h (Beardsley et al. 1985). Following, the velocity components were projected onto an along/cross-shore orthogonal coordinate system, with the positive alongshore axis oriented to the northeast (65°) and the positive cross-shore axis directed onshore, towards the southeast (155°).

The backscattered acoustic signal strength, from ADP, was also used to estimate SPM concentrations. After conversion to decibels, the signal strength was corrected for geometric spreading and water attenuation. Furthermore, an iterative approach (Kim et al. 2004) was used to also correct for sediment attenuation. The upper OBS-derived SPM concentration estimates were used to empirically calibrate the ADP's first bin. In general, the backscattering is affected by sediment type, size and composition. All are difficult to quantify by single frequency backscatter sensors (Hamilton et al. 1998). Limitations associated with optical and acoustic instruments have been addressed in literature (Voulgaris and Meyers 2004; Vincent et al. 2003; Fugate and Friedrichs 2002; Bunt et al. 1999; Hamilton et al. 1998; Thorne et al. 1991). Briefly, the optical sensors tend to underestimate the coarser particles present in the water column. Acoustic devices produce better estimates of mass concentration than optical for the coarser fraction (Fugate and Friedrichs 2002).

The flow data have been used to separate the records in different groups corresponding to different hydrodynamic forcing. All records collected correspond to a total of 380 full semi-diurnal tidal cycles. For each tidal cycle the average value of the alongshore low-passed flow was estimated and subsequently used to characterize the tidal cycle in terms of wind-driven flow (Table 2). All tidal cycles with an alongshore low-passed flow ranging from −0.05 to 0.05 m s^{-1} are considered to represent purely tidal forcing conditions; these are hereafter referred to as case 0 conditions (total of 173 tidal cycles, 46% of data). All remaining tidal cycles (203 cycles) with a low-passed alongshelf flow speed, in excess of 0.05 m s^{-1}, are assumed to correspond to periods with significant influence of wind-driven flows. Negative values correspond to flows towards the SW, driven by NE winds (case SWW, total of 100 cycles), while positive subtidal flows, in excess of 0.05 m s^{-1} (107 cycles), are directed to the NE, corresponding to wind forcing from the SW (case NEW). In addition to the above classification, each tidal cycle was classified as neap or spring, in terms of the tidal range of the particular cycle. Cycles with a tidal range greater than the mean range (3.6 m) are classified as spring tidal cycles, while cycles with a range less that 3.6 m as considered neap

Table 2 Data grouping in terms of wind forcing cases 0, SWW and NEW and tidal range (neap and spring) for each wind forcing case

Case	Subtidal flow (u_t)	Number of tidal cycles/%	Tidal range	Number of tidal cycles/%
Case 0 (tidal flow, no wind forcing)	$-0.05<u_t<0.05$ m s^{-1}	173/46	Neap	79/20.8
			Spring	94/24.7
Case SWW: (NE wind forcing)	$u_t<-0.05$ m s^{-1}	100/26	Neap	32/8.4
			Spring	68/17.9
Case NEW: (SW wind forcing)	$u_t>0.05$ m s^{-1}	107/28	Neap	58/15.3
			Spring	49/12.9
Total		380/100		380/100

tidal ranges. This classification has resulted in a total of six categories of tidal cycles where each category represents both tidal and wind forcing. Tidal cycles, from each category, were ensemble-averaged to create a "typical" representative tidal cycle for each case. Following the methodology described in Murphy and Voulgaris (2006) the time of data collection from each tidal cycle was converted from absolute time to tidal phase within the cycle, using the local high water slack time as a reference time. Then data from each case, falling within the same bin (width of 10 min) of the tidal phase, were averaged and a mean cycle and associated standard error were calculated.

3 Results

3.1 Wind and tidal circulation data

Wind and wave data were collected by a buoy (Flemish Government, Maritime Services, Coastal Division), located at 4 km from the BLA measurement location. The overall wind conditions over a period of 10 years and during the period of data collection is shown in Fig. 2. Wind analyses clearly show that winds from the SW are the strongest and most commonly occurring for 33% of the year. Cross-correlation with wave data, recorded by the buoy, indicates that these dominant winds from the SW coincide with an average wave height of 0.85 m and period of 4 s (Fig. 3).

For the three cases, the spring–neap tidal cycles for the near-bed (1.25 mab) alongshore and cross-shore currents are shown in Fig. 4a–f. Overall, the cross-shore components are negligible, indicating a highly rectilinear current ellipse, aligned with the coastline. Tidal forcing in the study area (case 0) is characterized by an asymmetry between ebb and flood. The maximum flood current is approximately 0.75 m s^{-1} and of short duration, while the ebb current peaks at 0.45 m s^{-1}, but persists longer in time; this is typical of asymmetrical tidal condition. Neap conditions show similar patterns in terms of asymmetry, but with reduced magnitudes.

Although, wind forcing was defined in terms of tidally averaged subtidal flow strength, the correlation between this flow and alongshore wind speed is used to check the assumption that these flows are predominantly (R^2=0.76) driven by the wind and not by baroclinic processes (Fig. 5). Case NEW corresponds with stronger winds than case SWW, something expected given the wind patterns in this area (see Fig. 2).

Examination of the tidal variability of the salinity records for each case reveals that overall salinity is highest (33) for case NEW and lowest (30.5) for case SWW; this indicates a higher riverine influence (Westerschelde) in the latter case (Fig. 6a–b). Steady winds bias the tidal forcing, because of the introduction of a wind-induced flow component. Fig. 4. (case SWW) shows that prevailing northeasterly winds result in increased ebb (33%) and slightly reduced flood current (15%), compared with the tidal forcing (case 0). These effects are most pronounced during spring tidal conditions. Southwesterly winds are the most common (case NEW) and tend to bias the ebb-flood current pattern significantly (Fig. 4e, f). Under spring conditions, the ebb current is reduced by 33%, whereas the flood current is enhanced by 13%.

3.2 SPM concentration and particle size

For the upper OBS (2 mab), the qualitative variation in SPM concentration is very similar for all cases (0, SWW, NEW). Generally, tidal variability is characterized by two local maxima, corresponding with ebb and flood flows, respectively, with the ebb maximum being lower than the one during flood (Fig. 7a–f). The flood is characterized by a

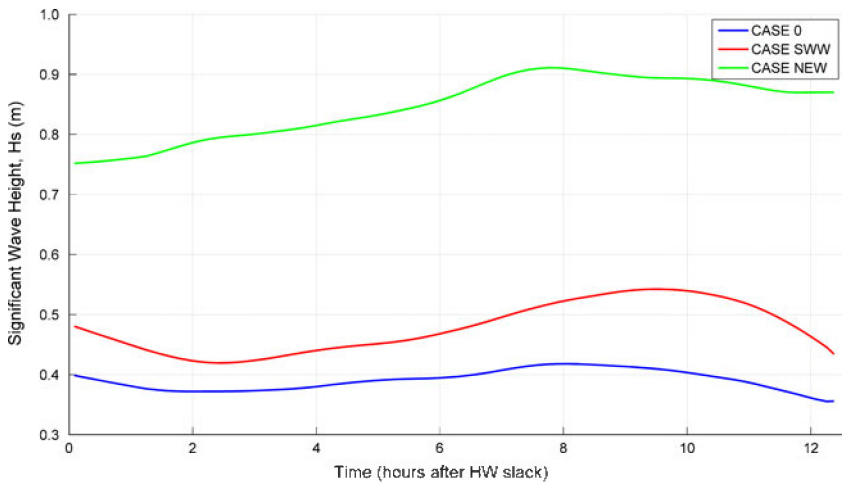

Fig. 3 Average significant wave height for the three cases under spring conditions. Highest waves occur in case NEW meteorological conditions

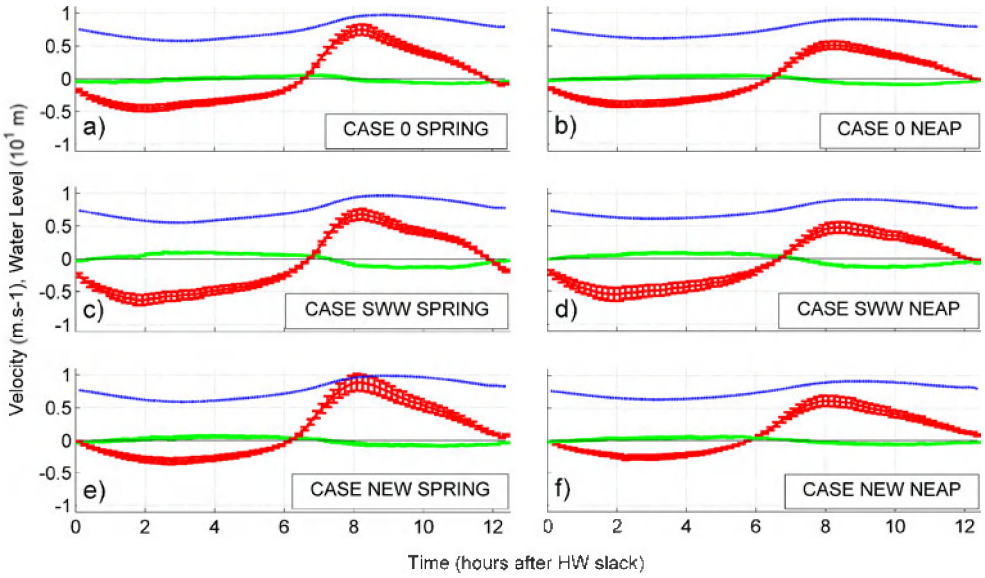

Fig. 4 Ensemble-averages of sea surface elevation (*blue*), alongshore (*red*) and cross-shore (*green*) currents derived from the ADP observations at 1.25 mab (m s^{-1}) for cases 0 (**a** and **b**), SWW (**c** and **d**) and NEW (**e** and **f**) and for spring (*left*) and neap (*right*) tidal range within each case. The *error bars* indicate standard error

pronounced maximum, occurring at the beginning of the flood during spring tide and is due to resuspension. This maximum is firstly detected at 0.2 mab and only later at 2 mab. The occurrence of such a time lag is well known and is related to the time necessary for vertical mixing (e.g. Bass et al. 2002). In cases 0 (Fig. 7a, b) and NEW (Fig. 7e, f) one can observe that around 2–3 and 9 h, when current strength is high, a vertical stratification of SPM concentration, according the two measuring levels, is limited. Vertical stratification remains always significant in case SWW (Fig. 7c, d), with permanently higher SPM concentrations present in the lower level than in the upper level.

The three cases show distinct differences in SPM concentration at 0.2 mab. Case SWW exhibits different maxima in SPM concentration during ebb as well as flood, indicating multiple resuspension events; whereas for case NEW the SPM concentration maximum occurs at the end of the ebb and during slack water. The remaining time SPM concentration is relatively low.

SPM concentrations, derived from ADP, are also plotted in Fig. 7. SPM concentration at 2 mab is very similar to the concentration derived from OBS, except during flood in case NEW. At 0.2 mab significant differences occur for case 0 and NEW (spring tides), where the ADP signal gives significantly higher SPM concentrations than the OBS. Under neap conditions, the OBS and ADP SPM data coincide well. Case SWW shows for both spring and neap conditions similar SPM concentrations at 0.2 mab for the OBS and ADP. These differences between optical and acoustic sensors are suggesting variability in sediment size composition that leads to different responses by the different sensors, something we will discuss later.

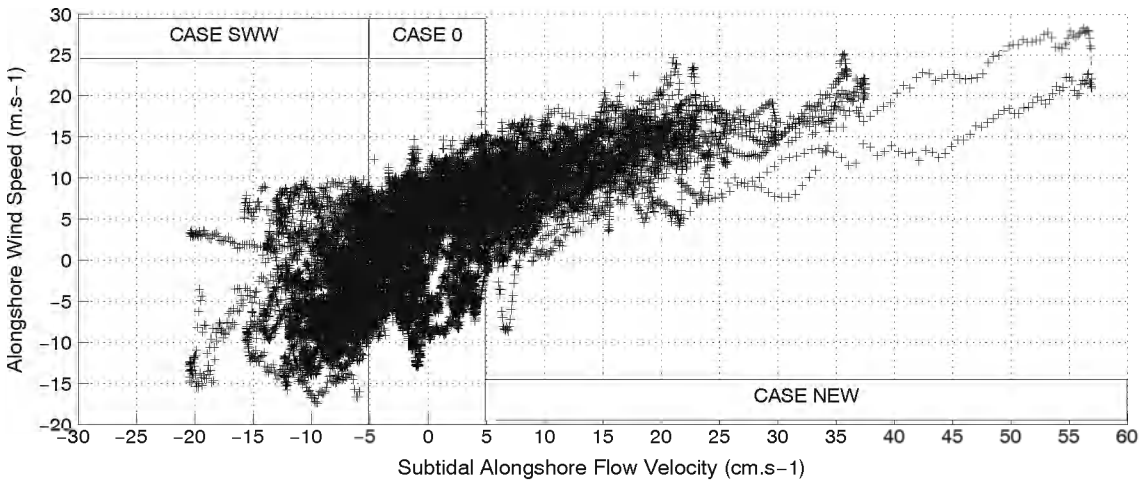

Fig. 5 Relationship between wind-induced flow in the alongshore direction and the alongshore wind component

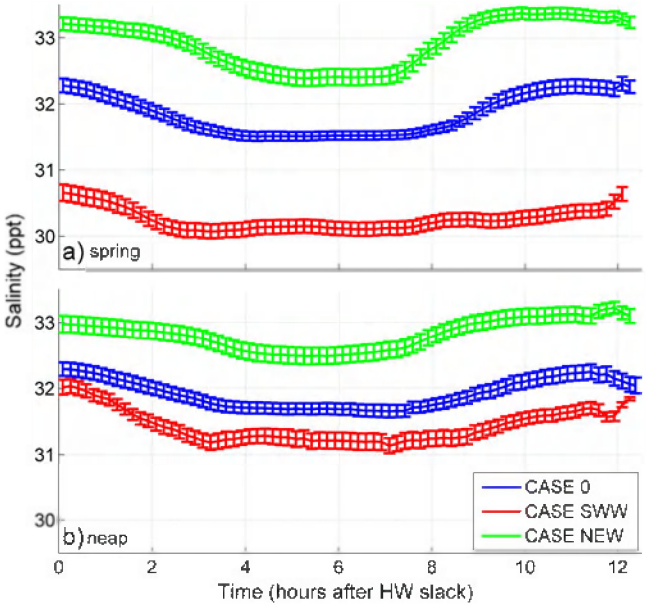

Fig. 6 Ensemble-averaged tidal variability of salinity measured at 1 mab for the three cases and for spring (*upper*) and neap (*lower*). The *error bars* indicate standard error

In situ particle sizes from LISST were classified and averaged per case (Fig. 8a–f). Overall, the median particle size varies between 40 and 130 μm. The fact that highest particle sizes occur during slack water and lowest during maximum velocities indicate that the main part of the particles consists of flocs. The median floc size in case SWW (Fig. 8c, d) is reduced during slack water (about 70 vs. 100 μm in case 0). Case NEW (Fig.8e, f) shows a distinct pattern with less pronounced particle size maxima. Higher standard error bars are because of more variable wave conditions occurring during case NEW.

3.3 Sea bed altimetry

Sea bed level variations have been derived from ADV altimetry. Besides the general procedure of averaging and grouping, a reference level has also been introduced in order to obtain normalised altimetry data from the five different tripod moorings taking into account the tripod movement (pitch and roll) and the dilute settling of the tripod into the sediment right after deployment and during high-energy meteorological events. The data per case (0, SWW, NEW) and per spring or neap condition are presented in Fig. 9(a–f). The sea bed level, on which the ADV acoustic signal reflects, might either consist of sandy material or strong SPM gradient when fluid mud or even HCMS is present.

For all cases (0, SWW, NEW), vertical bed level rises are associated with slack waters. Sea bed rise is on average 5 cm, under spring conditions, whereas during neap tides only a few cm. Case SWW (Fig. 9c, d) shows a clear sea bed rise during the HW slack (around 12 h).

4 Discussion

Measurements show that near-bed hydrodynamics and sediment dynamics, although dominated by the tidal forcing, are significantly modified by wind-induced flows

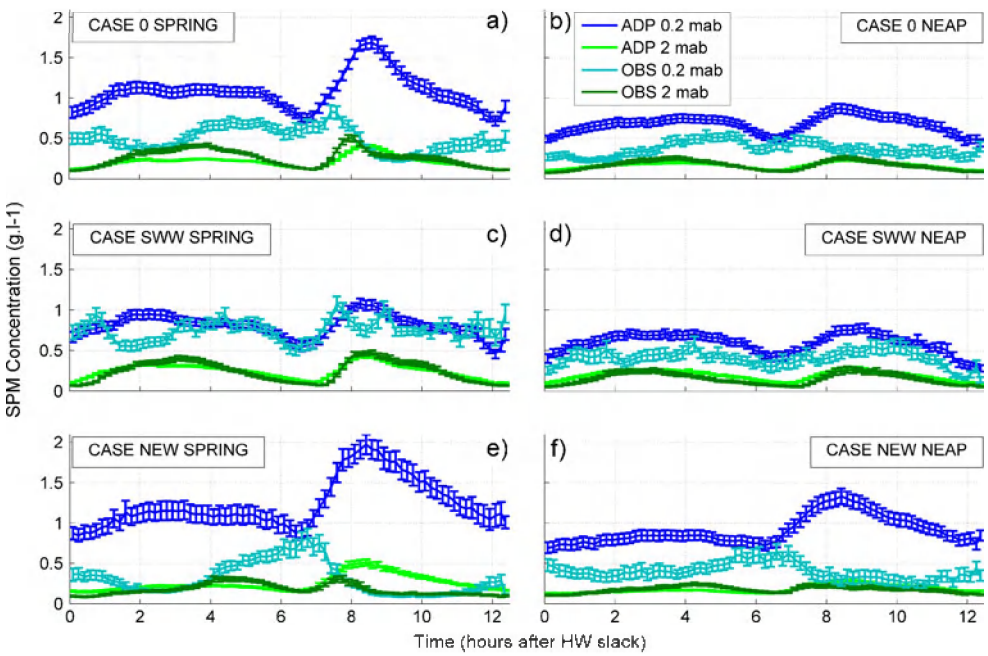

Fig. 7 Ensemble-averages of tidally varying SPM estimates from OBS and ADP at 0.2 (*blue*) and 2 mab (*green*). The *error bars* indicate standard error

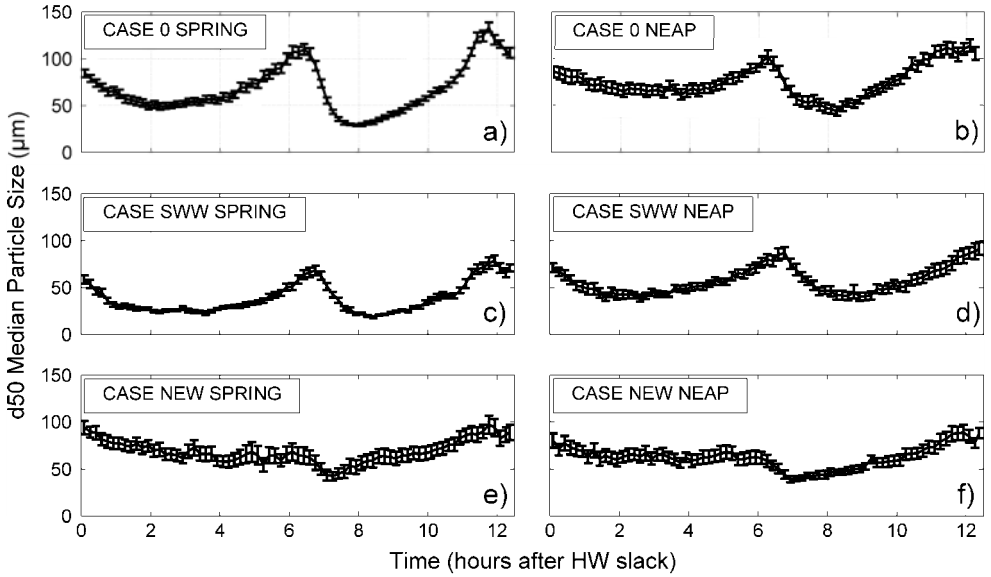

Fig. 8 Averaged median particle size as measured by the LISST 100X-type C. The *error bars* indicate standard error

with different effects, depending on the wind direction. Below the effects of wind and tidally driven circulation, as well as the distinct optical and acoustic response on varying SPM concentration and composition, are discussed in more detail. Furthermore, a conceptual sediment transport model is proposed for the area.

4.1 General tidal and wind-driven circulation in the study area

The wind climate in the study area is characterized by mainly SW and NE winds (Fig. 2, left–right) affecting the direction and strength of alongshore water mass transport. Salinity records are used as a proxy to identify the source of water masses (Fig. 6a–b). The salinity at the study site is mainly influenced by the Scheldt, Rhine and Seine rivers (Lacroix et al. 2004) and has an overall tidally and seasonally averaged mean of 32.2, with a standard deviation of 1.1. This salinity varies as a function of the tidal cycle. For periods of limited wind forcing (case 0) the mean salinity during ebb and flood amounts to 31.5 and 32.3, respectively. The mean salinity during periods associated with southwesterly winds (case NEW) is about 33, indicating advection of oceanic water masses from the English Channel towards the study site. On the other hand, during periods of NE wind activity (case SWW) the mean

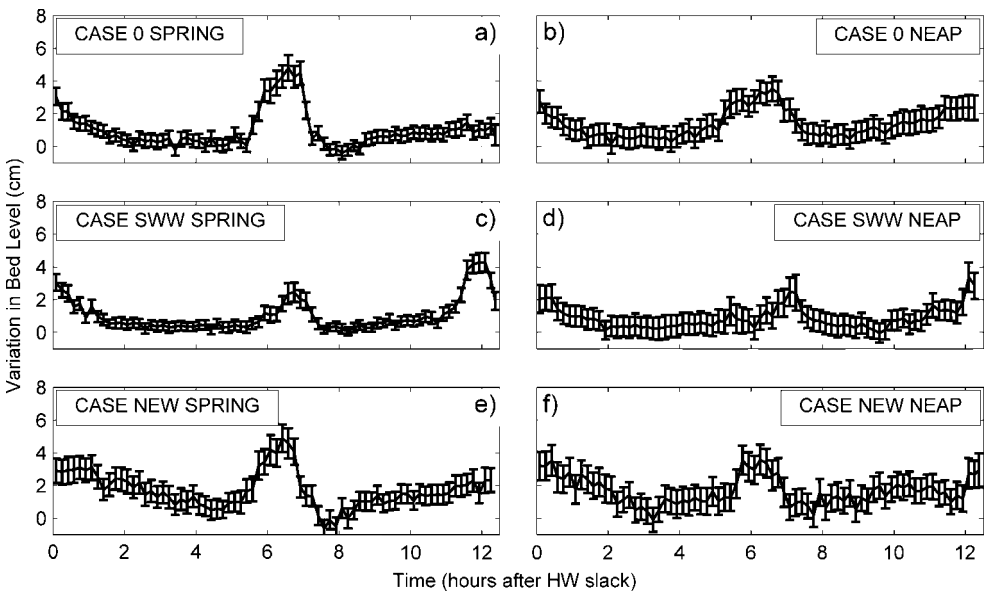

Fig. 9 Averaged sea bed level change derived from ADV altimetry with standard error bars

salinity reduces to 30.5, suggesting the influence of freshwater input, from mainly the Scheldt River, approximately 30 km away from the study site (Fig. 1).

SPM measurements, under tidal forcing only, show concentration maxima occurring at the end of ebb (5 h) and at the beginning of flood (8 h). The latter is a result of resuspension during maximum flood currents. The ebb-maxima are explained by the fact that the centre of the turbidity maximum is usually situated in ebb direction of the measurements. Hence, the maxima during ebb occur when, SPM concentrations advected from the centre of the turbidity maximum, have reached the measuring location. Neap tidal conditions show similar patterns, but with lower SPM concentrations. SPM measurements, from OBS, show that cases SWW (flow from NE) and NEW (flow from SW) correspond with high and lower SPM concentrations, respectively, and show that the wind-driven alongshore advection has a significant influence on SPM concentration. Indeed, ocean water masses, advected into the coastal area (case SWW), have generally lower SPM concentrations than the nearshore waters (Fettweis et al. 2010).

The ebb-flood tidal cycle is typically characterized by an increase and decrease in SPM concentration, driven by accelerating and decelerating currents, respectively. However, measurements indicate strikingly different SPM concentration behaviour near the bed (0.2 mab) between the three cases (Fig. 7a–f). The water column in the cases 0 (no wind-driven advection) and SWW (SW advection) is characterized by good vertical mixing, as can be seen in Fig. 7(a, b, e, and f) at about 2 and 9 h, when SPM concentration at 0.2 and 2 mab are very similar. However, in case NEW (advection from the SW) vertical mixing is sustained for a longer time interval (Fig. 7e, f). The vertical mixing during wind-driven advection from the NE (case SWW, Fig. 7c, d) is limited during both spring and neap tidal conditions; this is probably the result of higher mud concentrations and the occurrence of HCMS (see also below); the latter functioning as a bigger reservoir of sediment to be resuspended and thus maintaining a strong vertical gradient. The decreasing flows around 4 and 10 h favour settling of particles and results in a decrease of SPM concentration at 2 mab. However, a continuous increase in SPM concentration at 0.2 mab is only present in case NEW, where the maximum SPM concentration at 0.2 mab occurs around slack water. In cases 0 and SWW, the SPM concentration decreases around LW slack and HW slack, indicating the formation of HCMS near the bed. An extract (day of year (DOY) 130–144) from the time series (tripod mooring no. 5) of vertical distance between ADV sensor and sea bed boundary is shown in Fig. 10. Quarterdiurnal peaks of bed level change occur during slack water and consist of HCMS. They easily reach 10 cm with maxima of 15 cm, and last for at least 50 min (maximum of 3 h). The general sea bed level on which these changes are superimposed is also changing in time. Around DOY 136–140, a sea bed level change occurs under case SWW, spring conditions and persists over 4 days (~8 tidal cycles). This increase in bed level occurs during high vertical SPM concentration gradients and corresponds with the formation of HCMS.

In case NEW the SPM concentration is lower and wave conditions on average higher, resulting thus in less favourable conditions for deposition. Depending on how much sediment was deposited during slack water, a SPM concentration peak in both OBS's is shown during cases 0 and SWW (Fig. 7c, d).

4.2 Nature of sediment in resuspension

The nearshore area is characterized by the occurrence of fine sands (d50, 150 μm) and muds (Fettweis and Van den

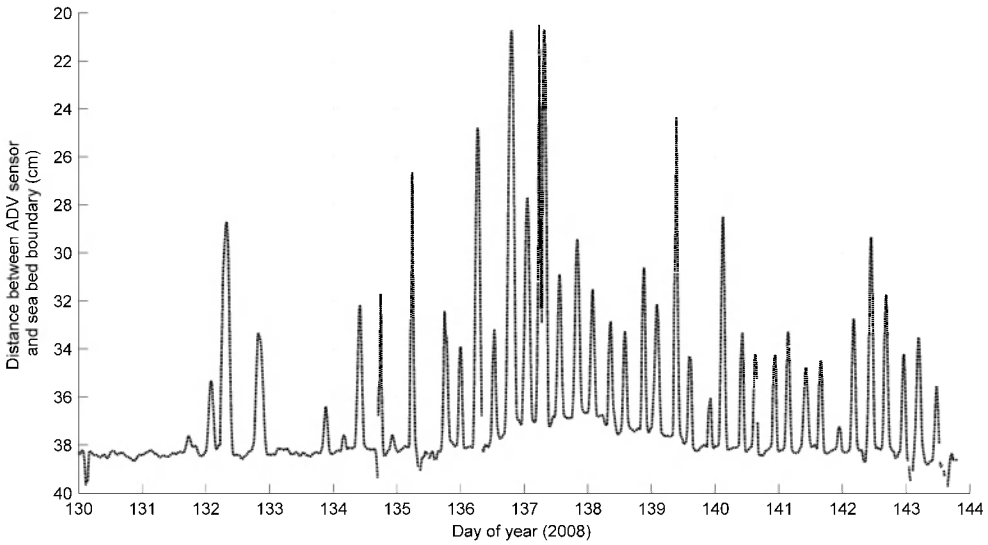

Fig. 10 Time-series of distance between ADV sensor and sea bed boundary (centimetre). Peaks indicate periodic deposits (quarterdiurnal). Around 136–140, a longer persisting HCMS/mud layer is present

Eynde 2003) suggesting that mixed sediment transport occurs. The wind-driven subtidal flow towards the NE (case NEW) increases the flood current on average by 13% and decreases ebb currents by 33%, compared with case I (Fig. 4a, b, e, f). The enhanced flood current is strong enough for resuspension of the in situ bed material. The measurements show that the OBS- and ADP-derived SPM concentrations are different, mostly during flood. Highest differences occur for case NEW (Fig. 7e, f), when flood currents are highest and reveal that SPM concentration, measured by the acoustic devices is significantly higher than by OBS. It is well known from literature that the OBS tends to underestimate the coarser particles in suspension (Downing 2006; Vincent et al. 2003; Voulgaris and Meyers 2004; Fugate and Friedrichs 2002; Bunt et al. 1999). This suggests that the higher SPM concentration, detected during flood, in the ADP is formed by the presence of fine sand in suspension. This is confirmed by the particle size data from the LISST (at 2 mab), showing a bimodal size distribution during maximum flood (Fig. 11). The first mode is situated around 35 μm and corresponds with the typical size of flocs (Fettweis et al. 2006) whereas the second mode corresponds with the median grain size of the sand (150 μm). The rising tail at fine particle sizes is due to the presence of particles finer than the measuring range of the instruments (Agrawal and Pottsmith 2000). The fact that flood currents are higher, that SPM concentrations are lower, and that the water column is well-mixed during case NEW, suggest that the parent bed (sand) is exposed and not covered with mud. The fact that the LISST does not detect sand-sized particles at 2 mab in the other cases suggests most probably that sand resuspension is lower; this is confirmed by the generally lower peak currents and the fact that the bed is during longer periods covered by mud (see below). As such, the data suggest the occurrence of an 'inverse' bed armouring, where a layer of fine sediments prevents the erosion of coarser material. Sand transport in the turbidity maximum area is therefore mainly directed in flood direction, with the highest sand transport rates during a wind-driven advection towards the NE.

4.3 Conceptual SPM transport system

Altimetry data (Figs. 9a–f and 10) show bed level variations that can be explained by the formation of HCMS. In case 0 and NEW (Fig. 9a, e) their occurrence is limited to slack water periods. The corresponding neap condition cases (Fig. 9b, f) show a similar, however, reduced pattern, as resuspension is lower. In case SWW (Figs. 9c, d and 10). the corresponding altimetry pattern suggests the occurrence of HCMS layers, persistent over several tides. Lower flood currents, together with higher SPM concentrations, a generally lower wave activity and a reduced vertical mixing strengthen the argument that a semi-permanent HCMS or mud layer is formed. The damping of turbulence by HCMS layers is a major mechanism maintaining these layers during longer time periods (Sheremet et al. 2005; Reed et al. 2009). Our data show that semi-permanent HCMS occur when the subtidal flow is directed towards the SW, mainly under NE wind forcing. These winds are not very frequent and their wind speeds are rather reduced. However, we believe that this type of benthic sediment transport is very important and has implications for object burial and sediment recirculation in and around the port (Fig. 1).

In case 0 and NEW, HCMS corresponds with deposition during slack water and resuspension by ebb-flood currents. We conclude that the variability in HCMS and SPM concentration is also influenced by shifts in the location

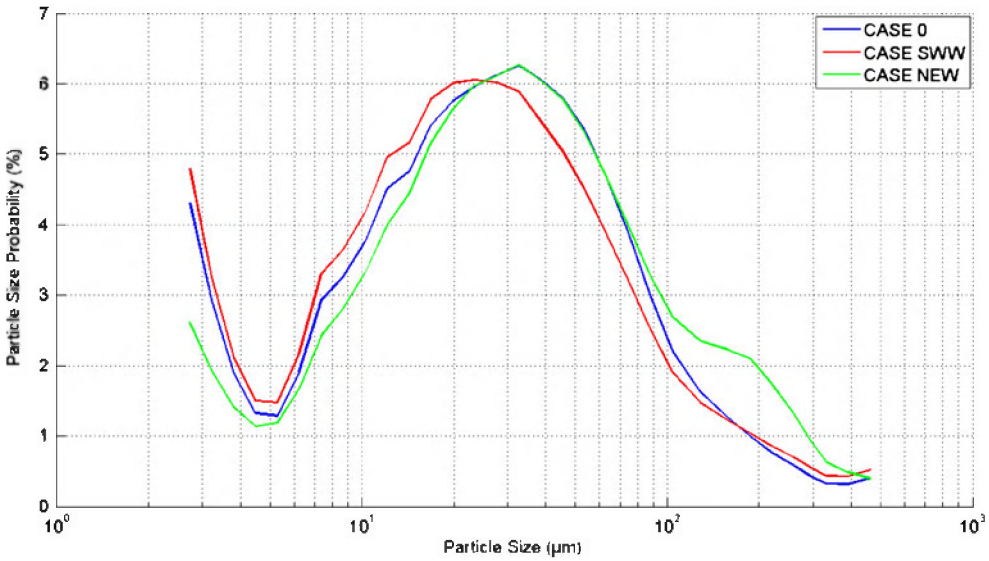

Fig. 11 Averaged particle size distributions around maximum flood current under spring conditions (8 h after HW slack, see Fig 7). Remark the bimodal distribution in case NEW, with one maximum around 45 μm and another one around 150–200 μm. The latter is caused by the resuspension of fine sand

of the high-turbidity maximum zone, which is controlled by the wind climate and thus alongshore advection. During case NEW, the TMZ is situated more towards the northeast and corresponds with SW winds (most frequent wind sector). For these conditions, no continuous HCMS was found. The parent bed consisting of fine sands will be exposed and resuspension of the parent bed can occur. Under these conditions, more marine fine-grained sediments are entering the Westerschelde estuary. Indeed, the Westerschelde cohesive sediments show a very strong marine signature (>80%) (Van Alphen 1990; Verlaan and Spanhoff 2000) suggesting that the estuary serves as a buffer of marine fine-grained matter (van der Wal et al. 2010). Part of these fine-grained sediments is permanently deposited in inter-tidal areas (Temmerman et al. 2003). The fact that under SW-directed subtidal flow, higher SPM concentrations are measured, suggests the outflow of marine sediments from the Westerschelde. Fettweis and Van den Eynde (2003) proposed that the turbidity maximum was formed by congestion in the sediment transport along the coast. Our data suggest also that the Westerschelde functions as storage area of marine sediments, which are released into the sea under specific hydro-meteo conditions.

5 Conclusions

A total of 198 days of in situ data on SPM and currents have been collected in the coastal turbidity maximum area of the Belgian inner shelf. The measurements, made in autumn–winter 2006–2007 and winter-spring 2008, were averaged and classified into three cases, based on the direction and strength of subtidal advection. The main conclusions are:

1. Near-bed hydrodynamics and SPM dynamics are predominantly dominated by tidal forcing. Generally, SPM concentration is significantly influenced by advection during ebb, whereas during flood local resuspension is more important.
2. A significant modification of the tidal forcing results from alongshore advection due to wind-induced flows and influences the position of the turbidity maximum; as such also the origin of SPM. Winds persistently blowing from the NE will increase SPM concentration, due to an increased SPM outflow from the Westerschelde estuary. SW winds will decrease SPM concentrations. The latter is related to the advection of less turbid English Channel water to the measuring location, inducing a shift of the turbidity maximum towards the NE and the Westerschelde estuary. Under these conditions, marine mud will be imported and buffered in the estuary.
3. With prevailing NE winds, the increase in SPM concentration results in the formation of persistent HCMS. The results have indicated that these layers mostly remain present throughout the tidal cycle. Inverse armouring occurs, as the sandy bed is sheltered from erosion. SPM consists of cohesive sediments only.
4. In case of tidal influence and SW prevailing winds, HCMS occur only around slack water. SPM consists of a mixture of cohesive sediments (flocs) and locally eroded sand grains during high currents.
5. Regarding instrumentation, it is shown that SPM estimates from OBS are only reliable when SPM consists of cohesive sediments only; with mixtures of cohesive and non-cohesive sediments, a combination of optical (OBS) and acoustic sensors (ADP, ADV) are needed to get an accurate estimate of the total SPM concentration.

Acknowledgements The study was partly funded by Belgian Science Policy (Science for a Sustainable Development, QUEST4D, SD/NS/06A) and partly by the Maritime Access Division of the Ministery of the Flemish Community (MOMO project). G. Dumon (Ministery of the Flemish Community, Maritime Services, Coastal Division/Hydrography) made available wind and wave measurement data. We want to acknowledge the crew of RV Belgica, Zeearend and Zeehond for their skilful mooring and recuperation of the tripod. Measurements would not have been possible without technical assistance of A. Pollentier, J.-P. De Blauwe, and J. Backers (Measuring service of MUMM, Oostende). The first author acknowledges a specialisation grant from IWT (Agency for Innovation by Science and Technology, Flanders)

References

Agrawal YC, Pottsmith HC (2000) Instruments for particle size and settling velocity observations in sediment transport. Mar Geol 168:89–114

Beardsley RC, Limeburner R, Rosenfeld LK (1985) Introduction to the CODE-2 moored array and large-scale data report. In: Limeburner R (ed) CODE-2: Moored array and large-scale data report. Tech Rep WHOI-85-35, Woods Hole Oceanogr Inst, Woods Hole, Mass, 234 pp

Bass SJ, Aldridge JN, McCave IN, Vincent CE (2002) Phase relationships between fine sedimens suspensions and tidal currents in coastal seas. J Geophys Res 107:C10–3146. doi:10.1029/2001JC001269

Bunt JAC, Larcombe P, Jago CF (1999) Quantifying the response of optical backscatter devices and transmissometers to variations in suspended particulate matter. Cont Shelf Res 19:1199–1220

Downing J (2006) Twenty-five years with OBS sensors: the good, the bad, and the ugly. Cont Shelf Res 26:2299–2318. doi:10.1016/j.csr.2006.07.018

Du Four I, Van Lancker V (2008) Changes of sedimentological patterns and morphological features due to the disposal of dredge spoil and the regeneration after cessation of the disposal activities. Mar Geol 255:15–29. doi:10.1016/j.margeo.2008.04.011

Fan D, Li C, Wang P (2004) Influences of storm erosion and deposition on rhythmites of the upper Wenchang Formation

(Upper Ordovician) around Tonglu, Zhejiang province, China. J Sediment Res 74:527–536. doi:10.1306/010304740527

Fettweis M, Van den Eynde D (2003) The mud deposits and the high turbidity in the Belgian-Dutch coastal zone, Southern bight of the North Sea. Cont Shelf Res 23:669–691. doi:10.1016/S0278-4343(03)00027-X

Fettweis M, Francken F, Pison V, Van den Eynde D (2006) Suspended particulate matter dynamics and aggregate sizes in a high turbidity area. Mar Geol 235:63–74. doi:10.1016/j.margeo.2006.10.005

Fettweis M, Nechad B, Van den Eynde D (2007) An estimate of the suspended particulate matter (SPM) transport in the southern North Sea using SeaWiFS images, in situ measurements and numerical model results. Cont Shelf Res 27:1568–1583. doi:10.1016/j.csr.2007.01.017

Fettweis M, Francken F, Van den Eynde D, Verwaest T, Janssens J, Van Lancker V (2010) Storm influence on SPM concentrations in a coastal turbidity maximum area with high anthropogenic impact (southern North Sea). Cont Shelf Res 30:1417–1427. doi:10.1016/j.csr.2010.05.001

Flemming BW, Delafontaine MT (2000) Mass physical properties of muddy intertidal sediments: some applications, misapplications and non-applications. Cont Shelf Res 20:1179–1197

Fugate DC, Friedrichs CT (2002) Determining concentration and fall velocity of estuarine particle populations using ADV, OBS and LISST. Cont Shelf Res 22:1867–1886

Hamilton LJ, Shi Z, Zhang SY (1998) Acoustic backscatter measurements of estuarine suspended cohesive sediment concentration profiles. J Coast Res 14:1213–1224

Lacroix G, Ruddick K, Ozer J, Lancelot C (2004) Modelling the impact of the Scheldt and Rhine/Meuse plumes on the salinity distribution in Belgian waters (southern North Sea). J Sea Res 52:149–163. doi:10.1016/j.seares.2004.01.003

Lauwaert B, Bekaert K, Berteloot M, De Backer A, Derweduwen J, Dujardin A, Fettweis M, Hillewaert H, Hoffman S, Hostens K, Ides S, Janssens J, Martens C, Michielsen T, Parmentier K, Van Hoey G, Verwaest T (2009) Synthesis report on the effects of dredged material disposal on the marine environment (licensing period 2008–2009). MUMM, ILVO, CD, aMT, WL report BL/2009/01, p. 73. Available at: http://www.mumm.ac.be/Downloads/News/synthesis_report_PW_2009.pdf

Kim HY, Gutierrez B, Nelson T, Dumars A, Maza M, Perales H, Voulgaris G (2004) Using the acoustic Doppler current profiler (ADCP) to estimate suspended sediment concentration. Technical Report CPSD #04-01.

Le Bot S, Lafite R, Fournier M, Baltzer A, Desprez M (2010) Morphological and sedimentary impacts and recovery on a mixed sandy to pebbly seabed exposed to marine aggregate extraction (eastern English Channel, France). Est, Coast Shelf Sci 89:221–233. doi:10.1016/j.ecss.2010.06.012

McAnally WH, Friedrichs C, Hamilton D, Hayter EJ, Shrestha P, Rodriguez H, Sheremet A, Teeter A (2007) Management of fluid mud in estuaries, bays, and lakes Present state of understanding on character and behavior. J Hydraul Eng 133:9–22. doi:10.1061/(ASCE)0733-9429 133:1(9)

Murphy S, Voulgaris G (2006) Identifying the role of tides, rainfall and seasonality in marsh sedimentation using long-ter, suspended sediment concentration data. Mar Geol 227:31–50. doi:10.1016/j.margeo.2005.10.006

Panagiotopoulos I, Voulgaris G, Collins MB (1997) The influence of clay on the threshold of movement of fine sandy beds. Coast Eng 32:19–43

PIANC (2008) Minimising harbour siltation, Report No 102, p. 75

Reed AH, Faas RW, Allison MA, Calliari LJ, Holland KT, O'Reilly SE, Vaughan WC, Alves A (2009) Characterization of a mud deposit offshore of the Patos Lagoon, southern Brazil. Cont Shelf Res 29:597–608. doi:10.1016/j.csr.2009.02.001

Sheremet A, Mehta AJ, Liu B, Stone GW (2005) Wave-sediment interaction on a muddy inner shelf during Hurricane Claudette. Est, Coast Shelf Sci 63:225–233. doi:10.1016/j.ecss.2004.11.017

Temmerman S, Govers G, Meire P, Wartel S (2003) Modelling long-term tidal marsh growth under changing tidal conditions and suspended sediment concentrations, Scheldt estuary, Belgium. Mar Geol 193:151–169

Torfs H, Mitchener H, Huysentruyt H, Toorman E (1996) Settling and consolidation of mud/sand mixtures. Coast Eng 29:27–45

Thorne PD, Hanes DM (2002) A review of acoustic measurement of small-scale sediment processes. Cont Shelf Res 22:603–632

Thorne PD, Vincent CE, Hardcastle PJ, Rehman S, Pearson ND (1991) Measuring suspended sediment concentrations using acoustic backscatter devices. Mar Geol 98:7–16

Van Alphen JSLJ (1990) A mud balance for Belgian-Dutch coastal waters between 1969 and 1986. Neth J Sea Res 25 (1/2):19–30

van der Wal D, van Kessel T, Eleveld MA, Vanlede J (2010) Spatial heterogeneity in estuarine mud dynamics. Oc Dyn 60:519–533. doi:10.1007/s10236-010-0271-9

Van Hoey G, Vincx M, Degraer S (2007) Temporal variability in the Abra alba community determined by global and local events. J Sea Res 58:144–155. doi:10.1016/j.seares.2007.02.007

Van Lancker VRM, Bonne W, Bellec V, Degrendele K, Garel E, Brière C, Van den Eynde D, Collins MB, Velegrakis AF (2010) Recommendations for the sustainable exploitation of tidal sandbanks. J Coast Res SI 51:151–64. doi:10.2112/SI51-014

van Ledden M, van Kesteren WGM, Winterwerp J (2004) A conceptual framework for the erosion behaviour of sand-mud mixtures. Cont Shelf Res 24:1–11. doi:10.1016/j.csr.2003.09.002

Velasco DW, Huhta CA (2010) Experimental verification of acoustic Doppler velocimeter (ADV) performance in fine-grained, high sediment concentration fluids. App Note SonTek/YSI

Verfaillie E, Van Meirvenne M, Van Lancker V (2006) Multivariate geostatistics for the predictive modelling of the surficial sand distribution in shelf seas. Cont Shelf Res 26:2454–2468. doi:10.1016/j.csr.2006.07.028

Verlaan PAJ, Spanhoff R (2000) Massive sedimentation events at the mouth of the Rotterdam waterway. J Coast Res 16:458–469

Vincent CE, Bass SJ, Rees JJ (2003) Uncertainties in suspended sediment concentration and transport due to variations in sediment size. In: Proceedings of Coastal Sediments '03, Clearwater, Florida, May 2002. p. 10

Voulgaris G, Meyers S (2004) Temporal variability of hydrodynamics, sediment concentration and sediment settling velocity in a tidal creek. Cont Shelf Res 24:1659–1683. doi:10.1016/j.csr.2004.05.006

Waeles B, Le Hir P, Lesueur P, Delsinne N (2007) Modelling sand/mud transport and morphodynamics in the Seine river mouth (France): an attempt using a process-based approach. Hydrobiol 588:69–82. doi:10.1007/s10750-007-0653-2

Wallbridge S, Voulgaris G, Tomlinson BN, Collins MB (1999) Initial motion and pivoting characteristics of sand partlicles in uniform and heterogeneous beds: experiments and modeling. Sedimentology 46:17–32

Wiberg PL, Drake DE, Cacchione DA (1994) Sediment resuspension and bed armoring during high bottom stress events on the northern California inner continental shelf: measurements and predictions. Cont Shelf Res 14:1191–1219

Williamson H, Torfs H (1996) Erosion of mud/sand mixtures. Coast Eng 29:1–25

Winterwerp JC (2005) Reducing harbour siltation I: methodology. J Waterw Port Coast Ocean Eng 131:258–266. doi:10.1061/(ASCE)0733-950X(2005)131:6(258)

Wu B, Molinas A, Shu A (2003) Fractional transport of sediment mixtures. Int J Sediment Res 18:232–247